Rotating Bose gas with hard-core repulsion in a quasi-two-dimensional harmonic trap: Vortices in Bose-Einstein condensates

M. A. H. Ahsan* and N. Kumar†
Raman Research Institute, Sir C. V. Raman Avenue, Bangalore 560080, India
(Received 14 November 2000; revised manuscript received 21 February 2001; published 31 May 2001)

We consider a gas of $N(\leqslant 15)$ Bose particles with hard-core repulsion, contained in a quasi-two-dimensional harmonic trap and subjected to an overall angular velocity Ω about the z axis. Exact diagonalization of the $n\times n$ many-body Hamiltonian matrix in given subspaces of the total (quantized) angular momentum L_z, with $n\sim 10^5$ (e.g., for $L_z=N=15$, $n=240\,782$) was carried out using Davidson's algorithm. The many-body variational ground-state wave function, as also the corresponding energy and the reduced one-particle density-matrix $\rho(\mathbf{r},\mathbf{r}')=\Sigma_\mu \lambda_\mu \chi_\mu^*(\mathbf{r})\chi_\mu(\mathbf{r}')$ were determined. With the usual identification of Ω as the Lagrange multiplier associated with L_z for a rotating system, the L_z-Ω phase diagram (or the stability line) was determined that gave a number of critical angular velocities Ω_{ci}, $i=1,2,3,\ldots$, at which the ground-state angular momentum and the associated condensate fraction, given by the largest eigenvalue of the reduced one-particle density matrix, undergo abrupt jumps. For a given N, a number of (total) angular momentum states were found to be stable at successively higher critical angular velocities Ω_{ci}, $i=1,2,3,\ldots$. All the states in the regime $N>L_z>0$ are metastable. For $L_z>N$, the L_z values for the stable ground states generally increased with increasing critical angular velocities Ω_{ci}, and the condensate was strongly depleted. The critical Ω_{ci} values, however, decreased with increasing interaction strength as well as the particle number, and were systematically greater than the nonvariational yrast-state values for the $L_z=N$ single vortex state. We have also observed that the condensate fraction for the single vortex state (as also for the higher vortex states) did not change significantly even as the two-body interaction strength was varied over several (~ 4) orders of magnitude in the moderately to the weakly interacting regime.

DOI: 10.1103/PhysRevA.64.013608 PACS number(s): 03.75.Fi, 67.40.−w, 05.30.Jp

I. INTRODUCTION

The experimental realization of Bose-Einstein Condensation (BEC) in dilute vapors of ultracold (nanokelvin) alkali atoms [1–3], and other systems [4], trapped in harmonic potential wells has qualitatively extended the domain of occurrence of the quantum fluids [5–7]. Unlike their dense and strongly interacting, homogeneous (bulk) counterparts, e.g., liquid ^{4}He, these mesoscopic gaseous systems are dilute, weakly or moderately interacting, and inhomogeneous—with controllable density, effective dimensionality, and tunable atom-atom interactions of either sign [8]. Further, the creation [10,9] of the vortex states with quantized circulation in externally rotated traps, as also the direct observation of phase coherence effects [11], have clearly revealed the phase rigidity characteristic of superfluidity associated with the BEC. The BEC in a weakly and repulsively interacting dilute Bose gas (i.e., with the two-body s-wave scattering length $a_{sc}\ll$ the mean interatomic spacing $\overline{n}^{-1/3}$, and with the number of atoms in the condensate $N\gg 1$) has often been described macroscopically through the Gross-Pitaevskii equation based on the condensate amplitude as a slowly varying order parameter [6]. Microscopic treatments going beyond the mean-field approximation and based on many-body variational wave functions also exist in the literature but involve heavy computations [12,13] even for the modest size of the system ($N\sim 10$–50). Besides, the existing mean field as well as many-body calculations involves only the ''Lowest Landau Level (LLL)'' single-particle orbitals, with only the positive sign (with respect to the trap angular velocity $\Omega\hat{e}_z$) of the single-particle angular momentum quantum number m. The interatomic repulsion is known to qualitatively change the ground-state properties of a system of weakly interacting neutral Bose gas (confined in a rotating harmonic trap) at $T=0$ in two distinct ways [6]. First, it leads to a depletion of the condensate fraction, which is equal to one for an ideal (noninteracting) Bose gas. Second, it gives a phase rigidity, or stiffness, to the ground-state many-body wave function. This is responsible for the superfluid flow that manifests in the successive appearance of vortices with higher quantized circulations beyond certain critical angular velocities Ω_{ci} of the rotating trap. Both these aspects are well described by the one-particle reduced density-matrix $\rho_1(\mathbf{r},\mathbf{r}')$ obtained from the N-body ground-state wave function $\Psi_0(\mathbf{r}_1,\ldots,\mathbf{r}_N)$ by partial integration, or tracing out, of the $N-1$ coordinates from the N-body pure density-matrix $\Psi_0^*(\mathbf{r}_1,\ldots,\mathbf{r}_N)\Psi_0(\mathbf{r}_1',\ldots,\mathbf{r}_N')$. (It is to be recalled in passing here that the condensate and the superfluid fractions are not the same thing. More specifically, e.g., for the nonrotating ground state of an interacting Bose gas at $T=0$, the condensate fraction is generally less than unity due to depletion while the superfluid fraction, that includes the condensate as well as the above-the-condensate fraction, is exactly equal to unity. Both the condensate, as well as the superfluid fractions, are characterized by the same quantum-

*Present address: Department of Physics, Indian Institute of Science, Bangalore 560 012, India.
†Email address: nkumar@rri.res.in

mechanical phase whose gradient gives the superfluid velocity. Also, both vanish together above the critical temperature T_c. In fact, it is the condensate that amplifies the effect of even the weakest repulsive interaction, leading to the absence of single-particle excitation and giving rise to the phase rigidity.)

In this work, we have studied the effect of the two-body repulsive interaction on the condensate fraction, and on the critical angular velocities (Ω_{ci}, $i=0,1,2,\ldots,$) for the appearance of different vortex states for a quasi-two-dimensional Bose gas confined in a highly anisotropic harmonic trap ($\omega_z \gg \omega_\perp$) subjected to an overall rotation Ω about the z axis. To this end, we use the many-body variational approach and calculate the ground-state energy, the ground-state wave function and the associated one-particle reduced density matrix for different values of the interaction, in given subspaces of the total quantized angular momentum L_z. The many-body variational ground-state wave function is obtained through the exact diagonalization of the $n\times n$ many-body Hamiltonian matrix (e.g., $n=240\,782$ for $L_z=N=15$) using Davidson's algorithm. A distinctive feature of the present work is that in constructing the many-body variational ground-state wave function in a given subspace L_z ($\equiv$ the eigenvalue corresponding to the z component of the total angular momentum operator $\hat{\mathbf{L}}_z$), we have included, in the configuration interaction, the one-particle states with the single-particle angular momentum ($\equiv\hat{\mathbf{l}}_z$) quantum number m of *either* sign, as also the higher ''Landau-Level (LL)'' states. One of our main results is the variation of the critical angular velocity Ω_{c1} with the interaction strength $\Lambda_2\equiv(N-1)\sqrt{2/\pi}a_{sc}/a_z$ (the meanings of various symbols will be given in the next section), namely, that not only does Ω_{c1} decrease with increasing Λ_2, it also stays systematically higher than its nonvarional value, e.g., that given by the relation $\Omega_{c1}=\omega_\perp(1-\Lambda_2/4)$ for the weakly interacting, dilute case [14,13,15]. We have also observed that the condensate fraction for the single vortex state with $L_z=N$ (as also for the higher vortex states) does not change significantly even if the two-body scattering length a_{sc} is changed over ~ 4 orders of magnitude in the moderately to the weakly interacting regime, namely, from $a_{sc}=1000a_0$ to $1a_0$, where a_0 is the Bohr radius.

This paper is organized as follows. In Sec. II, we present our model [18] and bring out, in passing, the mathematical analogy between the system under study here and the other well-known systems like in the Landau-Darwin-Fock problem, and argue that in a certain limiting case of interest to us here, it becomes essential to go beyond the lowest Landau Level (LLL) approximation so as to include higher LLs and with the single-particle angular momentum eigenvalue m taking both positive as well as negative values in constructing the many-body basis functions. Section III describes briefly the construction of the many-body basis functions and the determination of the variational ground-state wave function by diagonalizing the many-body Hamiltonian matrix using Davidson's algorithm. In Sec. IV, we outline the procedure for determining the critical angular velocities for the entry of the vortices into the system, and the determination of the one-particle reduced density-matrix characterizing the vortical state that gives various density profiles. Finally, in Sec. V, we present and discuss our results, and end the paper with a brief conclusion and future plan of work.

II. THE SYSTEM AND THE HAMILTONIAN

We begin by considering a system of interacting, spinless, particles (bosons) confined in an external harmonic potential (trap). The two-body interaction potential is, however, assumed to be gaussian in the particle-particle separation. The trap is also subjected to an externally impressed rotation at an angular velocity $\mathbf{\Omega}\equiv\Omega\hat{z}$. The Hamiltonian for the system in a frame corotating with the angular velocity $\mathbf{\Omega}$ is

$$\hat{\mathbf{H}}^{rot}=\hat{\mathbf{H}}^{lab}-\mathbf{\Omega}\cdot\hat{\mathbf{L}}^{lab},$$

$$\hat{\mathbf{H}}^{lab}=\sum_{i=1}^{N}\left[\frac{1}{2m}\left(\frac{\hbar}{i}\boldsymbol{\nabla}_i\right)^2+\frac{1}{2}m\omega_\perp^2(r_{\perp i}^2+\lambda_z^2 z_i^2)\right]+\frac{1}{2}\frac{4\pi\hbar^2 a_{sc}}{m}\left(\frac{1}{\sqrt{2\pi}\sigma}\right)^3\times\sum_{i\neq j}\exp^{-(1/2\sigma^2)\{(r_{\perp i}-r_{\perp j})^2+(z_i-z_j)^2\}},\qquad(1)$$

with

$$\hat{\mathbf{L}}_z^{lab}=\sum_{i=1}^{N}\hat{\mathbf{l}}_{z\,i}^{lab}=\frac{\hbar}{i}\sum_{i=1}^{N}(\mathbf{r}_i\times\boldsymbol{\nabla}_i)_z.$$

The coordinates $\{\mathbf{r}_i\}$ and the corresponding canonical momenta $\{(\hbar/i)\boldsymbol{\nabla}_i\}$ refer to the laboratory frame. Here, $\omega_\perp$ is the frequency of the harmonic confinement. From now onwards, we will drop the superscript *lab* on the Hamiltonian $\hat{\mathbf{H}}^{lab}$, the total angular momentum $\hat{\mathbf{L}}_z^{lab}$, the single-particle angular momentum $\hat{\mathbf{l}}_z^{lab}$, and their respective eigenvalues, and these will always be assumed to refer to the laboratory frame unless otherwise specified.

We now make the following assumptions. The confining asymmetric harmonic potential is highly oblate spheroidal, with $\lambda_z\equiv\omega_z/\omega_\perp\gg 1$, and hence, our confined system is effectively quasi-2D with the x-y rotational symmetry; the repulsive two-body scattering is dominantly in the s-wave channel with a scattering length a_{sc} and $4\pi\hbar^2 a_{sc}/m$ having the dimension of energy$\times$volume. The range σ of the two-body interaction is small enough compared to the interatomic spacing so as to effectively give a δ-function interaction potential $V(\mathbf{r},\mathbf{r}')=(4\pi\hbar^2 a_{sc}/m)\,\delta(\mathbf{r}-\mathbf{r}')$.

Now, for our N-body variational calculation we need to construct the N-body basis functions with proper symmetry. Since the system above is rotationally invariant in the x-y plane, the z component of the total angular momentum (L_z) is a good quantum number leading to block diagonalization of the Hamiltonian matrix into the subspaces of $\hat{\mathbf{L}}_z$. The N-body basis functions are, in turn, constructed as linear combinations of the symmetrized products of a finite number of single-particle basis-functions, which are chosen to be

eigenfunctions of the unperturbed single-particle Hamiltonian. With this in mind, let us consider the noninteracting single-particle Hamiltonian $\hat{\mathbf{h}}$ in the rotating frame, which we now separate into the z and the $(x$-$y)$-plane (commuting) components, $\hat{\mathbf{h}}_z$ and $\hat{\mathbf{h}}_\perp$, respectively:

$$\hat{\mathbf{h}}=\underbrace{\frac{1}{2m}\left(\frac{\hbar}{i}\boldsymbol{\nabla}_\perp\right)^2+\frac{1}{2}m\omega_\perp^2 r_\perp^2-\frac{\hbar}{i}\boldsymbol{\Omega}\cdot(\mathbf{r}_\perp\times\boldsymbol{\nabla}_\perp)}_{\mathbf{h}_\perp}$$

$$+\underbrace{\frac{1}{2m}\left(\frac{\hbar}{i}\boldsymbol{\nabla}_z\right)^2+\frac{1}{2}m\omega_z^2 z^2}_{\mathbf{h}_z}\equiv\mathbf{h}_\perp+\mathbf{h}_z. \tag{2}$$

The eigensolutions for $\hat{\mathbf{h}}_z$ are

$$\hat{\mathbf{h}}_z\mathbf{u}_{n_z}(z)=\epsilon_{n_z}\mathbf{u}_{n_z}(z),$$

where

$$\epsilon_{n_z}=\left(n_z+\frac{1}{2}\right)\hbar\omega_z,\quad n_z=0,1,2,\ldots,$$

$$\mathbf{u}_{n_z}(z)=\sqrt{\frac{\alpha_z}{\sqrt{\pi}2^{n_z}n_z!}}e^{-1/2\alpha_z^2z^2}H_{n_z}(\alpha_z z),$$

and

$$\alpha_z=\sqrt{m\omega_z/\hbar}$$

$\equiv$ inverse of the longitudinal oscillator length (a_z).

Here H_{n_z} is the Hermite polynomial. The system has been assumed to be quasi-2D in that there is practically no excitation along the relatively stiffer z axis, and hence, we set $n_z=0$.

Let us now consider $\hat{\mathbf{h}}_\perp$. With $\boldsymbol{\Omega}=\Omega\hat{e}_z$ and $\mathbf{r}_\perp=x\hat{e}_x+y\hat{e}_y$,

$$\hat{\mathbf{h}}_\perp\equiv\underbrace{-\frac{\hbar^2}{2m}\left[\frac{1}{r_\perp}\frac{\partial}{\partial r_\perp}\left(r_\perp\frac{\partial}{\partial r_\perp}\right)+\frac{1}{r_\perp^2}\frac{\partial^2}{\partial\phi^2}\right]+\frac{1}{2}m\omega_\perp^2 r_\perp^2}_{\hat{\mathcal{K}}_\perp}$$

$$-\Omega\hat{\mathbf{l}}_z\equiv\hat{\mathcal{K}}_\perp-\Omega\hat{\mathbf{l}}_z. \tag{3}$$

Here, $\hat{\mathcal{K}}_\perp$ is the single-particle 2D-harmonic oscillator Hamiltonian, for which the eigensolutions are known to be

$$\hat{\mathcal{K}}_\perp u_{n,m}(r_\perp,\phi)=\epsilon_{n,m}u_{n,m}(r_\perp,\phi),$$

$$\hat{l}_z u_{n,m}(r_\perp,\phi)=m\hbar\, u_{n,m}(r_\perp,\phi),$$

with

$$u_{n,m}(r_\perp,\phi)=\sqrt{\frac{\alpha_\perp^2}{\pi}\frac{\left(\frac{1}{2}[n-|m|]\right)!}{\left(\frac{1}{2}[n+|m|]\right)!}}$$

$$\times(r_\perp\alpha_\perp)^{|m|}e^{-1/2\alpha_\perp^2r_\perp^2}e^{im\phi}L_{1/2(n-|m|)}^{|m|}(\alpha_\perp^2r_\perp^2),$$

where

$$\alpha_\perp=\sqrt{m\omega_\perp/\hbar}$$

$\equiv$ the inverse of the transverse oscillator length $(a_\perp)$,

and

$$\epsilon_{n,m}=\Big(\underbrace{2n_r+|m|}_{n}+1\Big)\hbar\omega_\perp\equiv(n+1)\hbar\omega_\perp,$$

with

$$n_r=0,1,2,\ldots,\quad m=-\infty,\ldots,-1,0,+1,\ldots,+\infty,$$

or equivalently,

$$n=0,\ 1,\ 2,\ldots,\quad m=+n,\ +n-2,\ldots,-n+2,\ -n. \tag{4}$$

Here $L_{(1/2)(n-|m|)}^{|m|}(\alpha_\perp^2r_\perp^2)$ is the associated Laguerre polynomial. It may be noted in passing that the Hamiltonian in Eq. (2) can be readily generalized to include a charge q on the particle and an external magnetic-field **B** along the z axis. It then represents the well-known Landau-Darwin-Fock [16,17] problem in which $\zeta_\perp\equiv\sqrt{(qB/2m)^2+\omega_\perp^2}$ is now the frequency for the harmonic confining potential in the x-y-plane and $\varsigma\equiv(qB/2m+\Omega)$ is the cyclotron-rotational (or the centrifugal) angular velocity about the z axis [18]. Limiting to $n_r=0$ and taking $m=0,+1,+2,+3,\ldots$, in Eq. (4) corresponds to the ''lowest-Landau Level (LLL)'' approximation.

Let us examine the centrifugal/mechanical stability of the above system by rewriting $\hat{\mathbf{h}}_\perp$ as

$$\hat{\mathbf{h}}_\perp=\underbrace{\frac{1}{2m}\left(\frac{\hbar}{i}\boldsymbol{\nabla}_\perp-m(\boldsymbol{\Omega}\times\mathbf{r}_\perp)\right)^2}_{\hat{\mathcal{T}}}+\underbrace{\frac{1}{2}m\omega_\perp^2r_\perp^2-\frac{1}{2}m(\boldsymbol{\Omega}\times\mathbf{r}_\perp)^2}_{\hat{\mathcal{U}}}$$

$$\equiv\hat{\mathcal{T}}+\hat{\mathcal{U}}.$$

Here, $\hat{\mathcal{T}}$ is clearly a positive-definite operator. It can readily be shown that $\hat{\mathcal{U}}$ is negative definite, null, or positive definite, respectively, as $(\omega_\perp+\Omega)(\omega_\perp-\Omega)$ is negative, zero, or positive, respectively [18].

For $\hat{\mathcal{U}}$ negative definite, the Hamiltonian $\hat{\mathbf{h}}_\perp\equiv\hat{\mathcal{T}}+\hat{\mathcal{U}}$ is unbounded from below and there are no stable solutions. This situation arises for $\omega_\perp<\Omega$, i.e., when the rotational angular velocity Ω becomes larger than the confining harmonic trap frequency $\omega_\perp$.

For the special case of $\hat{\mathcal{U}}$ null, we have $\omega_\perp=\Omega$ and the Hamiltonian reduces to $\hat{\mathbf{h}}_\perp=\hat{\mathcal{K}}_\perp-\omega_\perp\hat{\mathbf{l}}_z$. This gives rise to a situation analogous to the Landau problem when the fre-

quency for the harmonic confinement is equal to the centrifugal frequency. Setting $\omega_\perp = 1/2\omega_c$, we have the eigenvalue equation

$$\hat{\mathbf{h}}_\perp \mathbf{u}_{n,m}(r_\perp,\phi) = (\hat{\mathcal{K}}_\perp - \omega_\perp \hat{\mathbf{l}}_z)\mathbf{u}_{n,m}(r_\perp,\phi) = (\epsilon_{n,m} - m\hbar\omega_\perp)\mathbf{u}_{n,m}(r_\perp,\phi),$$

with

$$(\epsilon_{n,m} - m\hbar\omega_\perp) = \left(\underbrace{n_r + \frac{1}{2}(|m|-m)}_{\mathcal{N}} + \frac{1}{2}\right)\hbar\omega_c \equiv \left(\mathcal{N} + \frac{1}{2}\right)\hbar\omega_c,$$

where

$$n_r = 0,1,2,3,\ldots,$$

and

$$m = -\infty\cdots -2,-1,0,+1,+2,\ldots,+\infty;$$

or equivalently

$$\mathcal{N} = 0,1,2,3,\ldots$$

and

$$m = -\mathcal{N},-(\mathcal{N}-1),\ldots,-2,-1,0,+1,+2,\ldots,+\infty. \tag{5}$$

Each of the $\mathcal{N}$ levels, the so-called Landau Levels (LLs), is infinitely degenerate corresponding to the infinitely many possible values of m. It is clear from the ordering of the single-particle energy levels (without interaction) in Eq. (5) that the single-particle states with positive m values (i.e., those with the angular momentum parallel to the overall rotational angular velocity $\mathbf{\Omega} \equiv \Omega \hat{e}_z$) are energetically favored. These states constitute a massively degenerate manifold. This is the usual rationale for using the positive m values only, in constructing the variational wave function for the Landau-like problem. This degeneracy for the special case of $\omega_\perp = \Omega$ is, however, lifted by the interparticle interactions.

Finally, we consider the physically interesting case of $\hat{\mathcal{U}}$ positive definite. The single-particle noninteracting Hamiltonian $\hat{\mathbf{h}}_\perp$, now becomes $\hat{\mathbf{h}}_\perp = \mathcal{K}_\perp - \Omega\hat{\mathbf{l}}_z$ with the eigenvalue solution:

$$\hat{\mathbf{h}}_\perp \mathbf{u}_{n,m}(r_\perp,\phi) = (\hat{\mathcal{K}}_\perp - \Omega\hat{\mathbf{l}}_z)\mathbf{u}_{n,m}(r_\perp,\phi) = (\epsilon_{n,m} - m\hbar\Omega)\mathbf{u}_{n,m}(r_\perp,\phi),$$

$$(\epsilon_{n,m} - m\hbar\Omega) = 2\left[n_r + \frac{1}{2}\left(|m| - m\frac{\Omega}{\omega_\perp}\right) + \frac{1}{2}\right]\hbar\omega_\perp,$$

where

$$n_r = 0,1,2,\ldots,$$

and

$$m = -\infty,\ldots,-2,-1,0,+1,+2,\ldots,+\infty. \tag{6}$$

In this physically relevant situation, the particle as observed in the rotating frame finds itself in a shallower harmonic potential of frequency $\sqrt{\omega_\perp^2 - \Omega^2}$, and the states will be more spread out. It can be seen from Eq. (6) that for the centrifugal frequency Ω significantly smaller than the confining frequency $\omega_\perp$, the degeneracy of the Landau levels is lifted even without interaction. Further, the interaction between the particles causes the different single-particle angular momentum states to scatter into each other. Thus, for the slowly rotating (low L_z) systems and for moderately, and *a fortiori* for strongly interacting systems, it may be necessary to include the single-particle basis functions with different values of n_r and with the angular momentum quantum number m taking both positive and negative values. This is the case we shall be concerned with in the following.

III. THE MANY-BODY VARIATIONAL WAVE FUNCTION

We need to perform the diagonalization of the Hamiltonian matrix in the subspaces of $\hat{\mathbf{L}}_z$ only. The N-body variational wave function $\Psi(\mathbf{r}_1,\ldots,\mathbf{r}_N)$ is a linear combination of the symmetrized products $\psi_b(\mathbf{r}_1,\mathbf{r}_2,\ldots,\mathbf{r}_N)$ of the one-particle basis functions $u_{n,m}(r_\perp,\phi)u_{n_z}(z) \equiv \underbrace{u_{n,m,n_z}(\mathbf{r})}_{\mathbf{n}} = u_{\mathbf{n}}(\mathbf{r})$ introduced earlier:

$$\Psi(\mathbf{r}_1,\mathbf{r}_2,\ldots,\mathbf{r}_N) = \sum_b C_b \psi_b(\mathbf{r}_1,\mathbf{r}_2,\ldots,\mathbf{r}_N)$$

with

$$\psi_b(\mathbf{r}_1,\mathbf{r}_2,\ldots,\mathbf{r}_N) = \frac{1}{\sqrt{N!}}\sum_P P\left(\frac{1}{\sqrt{\nu_\mathbf{0}!}}\prod_{i=1}^{\nu_\mathbf{0}} u_\mathbf{0}(\mathbf{r}_i)\frac{1}{\sqrt{\nu_\mathbf{1}!}} \times \prod_{i=\nu_\mathbf{0}+1}^{\nu_\mathbf{0}+\nu_\mathbf{1}} u_\mathbf{1}(\mathbf{r}_i)\cdots\frac{1}{\sqrt{\nu_\mathbf{k}!}}\prod_{i=\nu_\mathbf{0}+\nu_\mathbf{1}+\cdots+\nu_{\mathbf{k}-1}+1}^{\nu_\mathbf{0}+\nu_\mathbf{1}+\cdots+\nu_{\mathbf{k}-1}+\nu_\mathbf{k}} u_\mathbf{k}(\mathbf{r}_i)\right),$$

$$b \equiv (\nu_\mathbf{0},\nu_\mathbf{1},\ldots,\nu_\mathbf{j},\ldots,\nu_\mathbf{k}), \quad \sum_{\mathbf{j}=\mathbf{0}}^{\mathbf{k}} \nu_\mathbf{j} = N, \quad \sum_{\mathbf{j}=\mathbf{0}}^{\mathbf{k}} \nu_\mathbf{j} m_\mathbf{j} = L_z.$$

Here $\{C_b\}$ are the variational parameters, and P permutes the N particle coordinates. Also, $\nu_\mathbf{j}$ is the occupancy of the $\mathbf{j}$th single-particle basis function $(u_\mathbf{j})$. (It is to be remembered that the bold-faced single-particle index $\mathbf{j}$ stands for a set of single-particle quantum n, m, n_z.) The many-body quantum index b, labeling the many-body basis function $\psi_b(\mathbf{r}_1,\ldots,\mathbf{r}_N)$, stands for a set of single-particle quantum numbers required to satisfy the above two defining relations between the single-particle occupation quantum numbers $\{\nu_\mathbf{j}\}$, the single-particle angular momentum quantum numbers $\{m_\mathbf{j}\}$, the number of particles N and the total angular momentum L_z. At this point it becomes more convenient to

switch over to second-quantization notation in the occupation number ($\nu_{\mathbf{j}}$) representation. The basis function is then

$$|\psi_b\rangle \equiv \frac{(a_{\mathbf{0}}^{\dagger})^{\nu_{\mathbf{0}}}(a_{\mathbf{1}}^{\dagger})^{\nu_{\mathbf{1}}}(a_{\mathbf{2}}^{\dagger})^{\nu_{\mathbf{2}}}\cdots(a_{\mathbf{k}}^{\dagger})^{\nu_{\mathbf{k}}}}{\sqrt{\nu_{\mathbf{0}}!\,\nu_{\mathbf{1}}!\quad\nu_{\mathbf{2}}!\cdots\nu_{\mathbf{k}}}}|0\rangle$$

$$\equiv \left| (\nu_{\mathbf{0}}\nu_{\mathbf{1}}\cdots\nu_{\mathbf{k}}) : \sum_{\mathbf{j}=\mathbf{0}}^{\mathbf{k}} \nu_{\mathbf{j}} = N, \quad \sum_{\mathbf{j}=\mathbf{0}}^{\mathbf{k}} \nu_{\mathbf{j}} m_{\mathbf{j}} = L_z \right\rangle, \quad (7)$$

with

$$\sum_{\mathbf{j}=\mathbf{0}}^{\mathbf{k}} \nu_{\mathbf{j}} = N, \quad \sum_{\mathbf{j}=\mathbf{0}}^{\mathbf{k}} \nu_{\mathbf{j}} m_{\mathbf{j}} = L_z$$

and the many-body Hamiltonian written in the second-quantized notation is

$$\mathbf{H} = \sum_{\mathbf{i},\mathbf{j}} \langle \mathbf{i}|1|\mathbf{j}\rangle a_{\mathbf{i}}^{\dagger} a_{\mathbf{j}} + \frac{1}{2}\sum_{\mathbf{i}_1,\mathbf{j}_1} \sum_{\mathbf{i}_2,\mathbf{j}_2} \langle \mathbf{i}_1,\mathbf{i}_2|2|\mathbf{j}_1,\mathbf{j}_2\rangle \times (a_{\mathbf{i}_1}^{\dagger} a_{\mathbf{j}_1} a_{\mathbf{i}_2}^{\dagger} a_{\mathbf{j}_2} - \delta_{\mathbf{i}_2\mathbf{j}_1} a_{\mathbf{i}_1}^{\dagger} a_{\mathbf{j}_2}).$$

Here, $a_{\mathbf{j}}^{\dagger}(a_{\mathbf{j}})$ are the usual bosonic creation (annihilation) operators, and $\langle \mathbf{i}|1|\mathbf{j}\rangle$ and $\langle \mathbf{i}_1,\mathbf{i}_2|2|\mathbf{j}_1,\mathbf{j}_2\rangle$ are the one-body and the two-body matrix-elements, respectively, over the single-particle basis functions. The evaluation of the matrix elements for the kinetic energy and the harmonic trapping potential over the single-particle basis chosen in the previous section is trivial. It is also possible to obtain closed form expressions for the matrix elements for the two-body (as also for the n body, $n=2,3,\ldots$) Gaussian potential(s) over the above basis as they reduce to multidimensional Gaussian integrals. (In the calculations presented here, however, we have not considered the three or the higher-body potentials.)

The variational parameters $\{C_b^0\}$ for the ground-state wave function $\Psi_0 = \Sigma_b C_b^0 \psi_b$ are now determined by minimizing $K_0\{\Psi_0\} \equiv \langle \Psi_0|\mathbf{H}|\Psi_0\rangle - E_0\langle \Psi_0|\Psi_0\rangle$ with respect to Ψ_0. The Lagrange multiplier E_0 will be identified as the variational energy for the ground state. The ith excited state $\Psi_i = \Sigma_b C_b^i \psi_b$ is determined by carrying out the variational minimization in the restricted Hilbert subspace that is orthogonal to the $(i-1)$ states determined earlier, i.e., by minimizing $K_i\{\Psi_i\} \equiv \langle \Psi_i|\mathbf{H}|\Psi_i\rangle - E_i\langle \Psi_i|\Psi_i\rangle$ with $\langle \Psi_j|\Psi_i\rangle = 0$ for $j=0,1,\ldots,(i-1)$.

The Davidson algorithm of iterative diagonalization [19] is based on a procedure where one keeps a minimum set of i orthogonal, trial wave functions that span a small subspace $\mathcal{S}_i$ of the full many-body Hilbert space:

$$\mathcal{S}_i \equiv \left\{ \Psi_j | \Psi_j = \sum_b C_b^j \psi_b, \quad j=0,1,\ldots,i \right.$$

and

$$\langle \Psi_j|\Psi_k\rangle = \delta_{jk}$$

for

$$\left. j,k=0,1,\ldots,i \right\}.$$

This small subspace $\mathcal{S}_i$ is chosen to contain dominant contributions from the ground state and the first few excited states. An $i\times i$ representation $H^{(i)}$ of the Hamiltonian $\mathbf{H}$ is obtained over this small subspace to set up the small eigenvalue equation $H^{(i)}\mathbf{a}_{\nu} = \lambda_{\nu}^{i}\mathbf{a}_{\nu}$, $\nu=0,1,2,\ldots,i$. $H^{(i)}$ is an effective Hamiltonian for the system over the small subspace $\mathcal{S}_i$ spanned by $\{\Psi_j,\ j=0,1,2,\ldots,i\}$. The eigenvalue λ_{ν}^{i} is the νth approximate eigenvalue. The convergence for the νth state is achieved when the residual vector for the νth state $|\Delta\Psi_{\nu}\rangle = \mathbf{H}|\Psi_{\nu}\rangle - \lambda_{\nu}^{i}|\Psi_{\nu}\rangle$ becomes a null vector. If the convergence has not been achieved, the residual vector $\Delta\Psi_{\nu}$, after orthonormalization, is added to the list of trial vectors to augment the subspace $\mathcal{S}_i$ to obtain $\mathcal{S}_{i+1} = \{\Psi_j,\ j=0,1,2,\ldots,i+1\}$. The procedure is continued till the convergence is obtained. In the process, if the size of the subspace $\mathcal{S}_i$ becomes unwieldingly large, a certain number of higher eigenvectors are dropped from $\mathcal{S}_i$ and the procedure once again initiated.

For $N=15$ particles, for example, we have carried out calculations for all the total angular momentum states in the regime $0 \leqslant L_z \leqslant 3N$. Diagonalization of the Hamiltonian matrix is performed for each of the subspaces of L_z separately. [We have set $n_z=0$ in the single-particle basis function $u_{n_z}(z)$ for reasons discussed earlier.] The single-particle basis $u_{n,m}(r_{\perp},\phi)$ with $n \equiv 2n_r + |m|$ $n_r = 0,1,\ldots,$ and $|m| = 0,1,2,\ldots,$ spanning the 2D x-y plane for a given subspace of L_z, is chosen as follows. It is convenient to define $l \equiv [L_z/N]$, where for real x, the symbol $[x]$ denotes the greatest integer less than or equal to x. For very weakly interacting particles, almost all the particles will condense into a single one-particle state $n=m=l$ a yrast-like state. As the interaction becomes stronger, the particles start scattering out to other single-particle states around this state, i.e., some of the particles go to states with higher angular momentum while some of them go to states with lower angular momentum (the two-body interaction conserves the total angular momentum). The single-particle angular momentum for the basis functions is now chosen to be: $m = l - n_b,\ l - n_b + 1, \ldots, l + n_b - 1,\ l + n_b$, where n_b is some positive integer that we have chosen to be 3, 4, or more depending on the strength of the interaction and the computational resources available (n_b is a kind of the size of the single-particle basis chosen for the calculation for a given value of L_z and describes configurational interaction). In all our calculations presented here we have taken $n_r = 0,\ 1$, and $n_b = 3$. Thus, for example, for $N=15$ and for the chosen subspace $L_z = 33$, we get $l \equiv [L_z/N] = 2$, and the single-particle angular momentum quantum number takes values $m = -1,0,+1,+2,+3,+4,+5$. Then, with $n_r = 0,1$, the single-particle basis set turns out to be

$$\{u_{0,0},\ u_{1,+1},\ u_{2,+2},\ u_{3,+3},\ u_{4,+4},\ u_{5,+5},\ u_{1,-1},\ u_{2,0},\ u_{3,+1},\ u_{4,+2},\ u_{5,+3},\ u_{3,-1}\}.$$

Thus, the $N(=15)$-body basis functions $\{\psi_b\}$, for the $L_z = 33$ subspace, are to be constructed from these single-particle basis functions. These were used in turn to construct

the variational trial function $\Psi=\Sigma_b C_b\psi_b$, and the ground state properties for the given value of L_z.

IV. CRITICAL ANGULAR VELOCITIES AND THE ONE-PARTICLE DENSITY MATRIX FOR THE CONFINED ROTATING BOSE GAS AT ZERO TEMPERATURE

From the variational ground-state wave function $\Psi_0(\mathbf{r}_1,\ldots,\mathbf{r}_N)$ obtained in the previous section, we now, in the following, go on to calculate various quantities of interest.

Let us first calculate the critical angular velocities $\{\Omega_{ci}\}$ for the onset of different vortical states. Note that for a system of N particles confined in a trap rotating at an angular velocity Ω, the thermodynamic equilibrium corresponds to the minimum of the free energy F given by $\exp\{-\beta F\}=\mathrm{Tr}[\exp\{-\beta(\hat{\mathbf{H}}^{lab}-\hbar\Omega\hat{L}_z^{lab})\}]$, where $\hat{\mathbf{H}}^{lab}-\hbar\Omega\hat{\mathbf{L}}_z^{lab}\equiv\hat{\mathbf{H}}^{rot}(\Omega)$, as we have noted earlier, is the Hamiltonian of the system in the corotating frame. For a system at $T=0$, the expression for the free energy reduces to a simpler form $F=\langle\Psi_0|(\hat{\mathbf{H}}^{lab}-\hbar\Omega\hat{\mathbf{L}}_z^{lab})|\Psi_0\rangle=\langle\hat{\mathbf{H}}^{lab}\rangle-\hbar\Omega\langle\hat{\mathbf{L}}_z^{lab}\rangle$ where Ψ_0 is the ground-state wave function of the system in the laboratory frame for a given value of L_z obtained, in our case, variationally. The above relation can be seen as the minimization of the energy $\langle\hat{\mathbf{H}}^{lab}\rangle\equiv E_0^{lab}$ subject to the constraint that the system has the angular momentum expectation value $\langle\hat{\mathbf{L}}_z^{lab}\rangle$. The angular velocity Ω is then the corresponding Lagrange multiplier. Since we have constructed our variational wave function Ψ_0 to be an eigenfunction of the total angular momentum operator $\hat{\mathbf{L}}_z^{lab}$, we will necessarily have $\langle\hat{\mathbf{L}}_z^{lab}\rangle=L_z$. Initially, when the system is subjected to no external rotation, the angular momentum state $L_z=0$ corresponds to the ground state of the system. As the system is rotated, other nonzero angular momentum states ($L_z\neq 0$) successively become the ground state of the system. These are obtained by minimizing the energy $E_0^{rot}(L_z,\Omega,\Lambda_2)$ in the rotating frame:

$$E_0^{rot}(L_z,\Omega,\Lambda_2)\equiv E_0^{lab}(L_z,\Lambda_2)-\hbar\Omega L_z^{lab}. \tag{8}$$

Here, Λ_2 measures the two-body interaction strength and has been defined in Sec. I. Thus, the critical angular velocity Ω_c beyond which the higher angular momentum state L_z, say, becomes lower in energy in the rotating frame compared to the lower angular momentum state $L_z'(<L_z)$ is given by

$$\Omega_c=\frac{E_0^{lab}(L_z,\Lambda_2)-E_0^{lab}(L_z',\Lambda_2)}{(L_z-L_z')\hbar}. \tag{9}$$

This gives us a number of critical angular velocities $\{\Omega_{ci},\ i=0,1,2,\ldots\}$ at which the ground state of the rotating system changes its angular momentum state abruptly. The angular momentum L_z of the ground state *versus* the angular velocity Ω relation, called the L_z-Ω phase diagram, or the stability line, for the rotating system was calculated in terms of the variational ground states obtained. We present this in Fig. 1 for $N=15$ system in the angular momentum regime $0\leqslant L_z\leqslant 3N$.

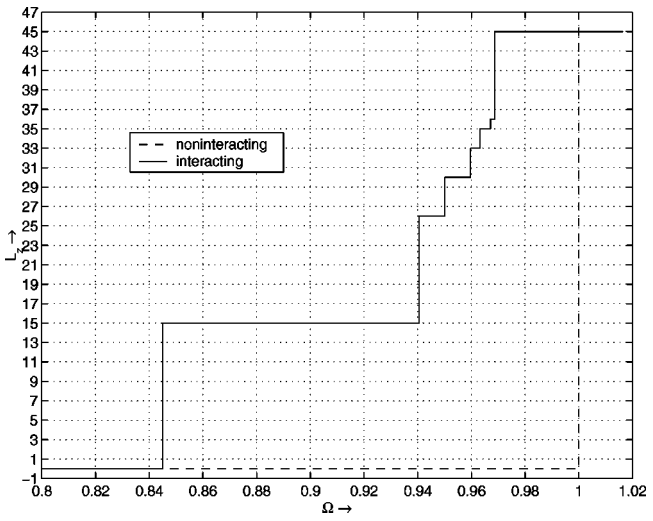

FIG. 1. Gives the plot (solid line) for the total angular momentum L_z in units of $\hbar$ versus the critical rotational velocity Ω_{ci} (in units of $\omega_\perp$) for the rotating BEC. Dashed line is for the noninteracting case, included here for reference.

Next, we calculate the one-particle reduced density matrix. From the many-body ground-state wave function $\Psi_0(\mathbf{r}_1,\ldots,\mathbf{r}_N)$, obtained through the variational exact diagonalization (ED), the one-particle reduced density matrix $\rho_1(\mathbf{r},\mathbf{r}')$ is obtained by integrating out the $N-1$ coordinates:

$$\rho_1(\mathbf{r},\mathbf{r}')\equiv\int\int\cdots\int d\mathbf{r}_2 d\mathbf{r}_3\cdots d\mathbf{r}_N\Psi_0^*(\mathbf{r},\mathbf{r}_2,\mathbf{r}_2,\ldots,\mathbf{r}_N)\Psi_0(\mathbf{r}',\mathbf{r}_2,\mathbf{r}_3,\ldots,\mathbf{r}_N)$$

$$=\sum_n\sum_m\sum_{n_z}\sum_{n'}\sum_{m'}\sum_{n_z'}\rho_{nmn_z,n'm'n_z'}u^*_{n,m,n_z}(\mathbf{r})u_{n',m',n_z'}(\mathbf{r}')$$

$$\equiv\sum_\mu\lambda_\mu\chi^*_\mu(\mathbf{r})\chi_\mu(\mathbf{r}')\quad(1\geqslant\lambda_1\geqslant\lambda_2\geqslant\lambda_3\geqslant\cdots\lambda_\mu\geqslant\cdots\geqslant 0)$$

$$=\underbrace{\lambda_1\chi_1^*(\mathbf{r})\chi_1(\mathbf{r}')}_{\rho_1^{(1)}(\mathbf{r},\mathbf{r}')}+\underbrace{\lambda_2\chi_2^*(\mathbf{r})\chi_2(\mathbf{r}')}_{\rho_1^{(2)}(\mathbf{r},\mathbf{r}')}+\underbrace{\sum_{\mu=3}\lambda_\mu\chi_\mu^*(\mathbf{r})\chi_\mu(\mathbf{r}')}_{\rho_1^{(\mu>2)}(\mathbf{r},\mathbf{r}')}$$

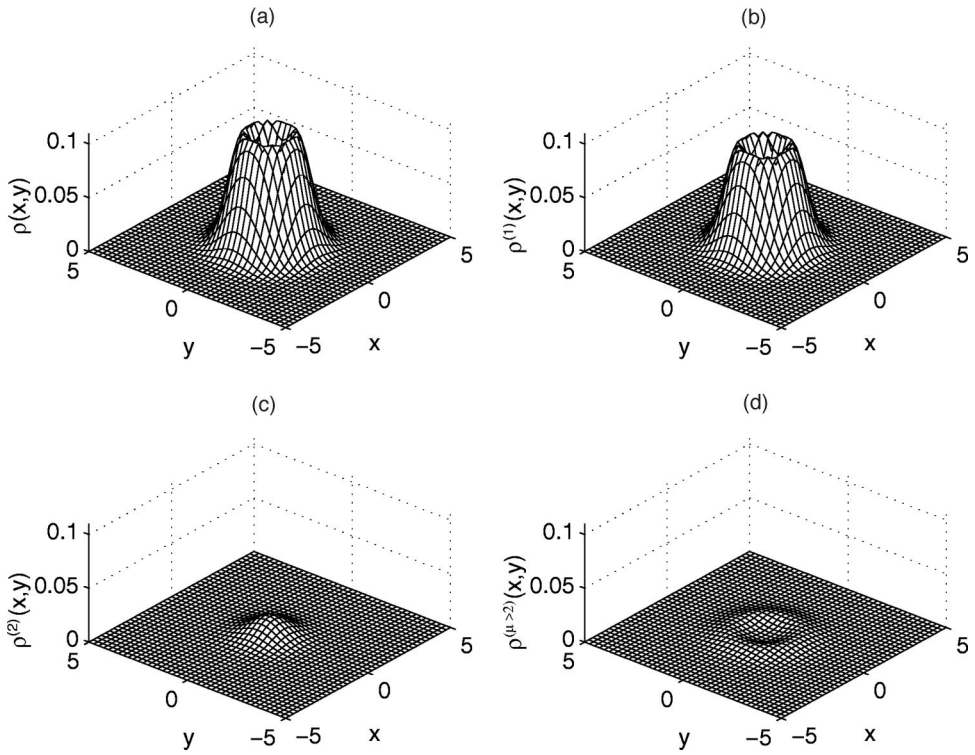

FIG. 2. Depicts the normalized particle density in units of $a_\perp^{-2}$ for (a) the total system $\rho(r_\perp)$, (b) the condensate fraction $\rho^{(1)}(r_\perp)$, (c) the nonrotating component $\rho^{(2)}(r_\perp)$, and (d) the remaining components $\rho^{(\mu>2)}(r_\perp)$ in the x-y plane. Distances are in units of $a_\perp$.

with

$$\chi_\mu(\mathbf{r}) \equiv \sum_n \sum_m \sum_{n_z} c^\mu_{n,m,n_z} u_{n,m,n_z}(\mathbf{r})$$

and

$$\sum_\mu \lambda_\mu = 1, \tag{10}$$

where $\{\lambda_\mu\}$ are the eigenvalues and $\{\chi_\mu(\mathbf{r})\}$ the corresponding eigenvectors of the one-particle reduced density-matrix $\rho_1(\mathbf{r},\mathbf{r}')$. We have ordered, in the above equation, the eigenvectors of the density matrix according as the nondecreasing values of the corresponding eigenvalues. We have also resolved the density matrix in a certain way for reasons that will become clear in the next section when we present various density plots in Figs. 2 and 3. The diagonal part $\rho_1(\mathbf{r},\mathbf{r}) \equiv \rho(\mathbf{r})$ gives the single-particle density profile of the system. For our finite system, the BEC corresponds to a single eigenvalue λ_1 being significantly larger than the rest of the eigenvalues and the corresponding eigenvector $\chi_1(\mathbf{r})$ is the counterpart of the macroscopic order parameter $\phi(\mathbf{r})$ obtained from the solution of the Gross-Pitaevskii equation with λ_1 being identified as the condensate fraction and m_1 the vorticity of the condensate. As noted before, our system is quasi-2D, and hence we set $n_z = 0$ and the summation over n_z in Eq. (10) goes off. We also observe that $\chi_\mu(\mathbf{r})$ is an eigenvector of the single-particle angular momentum $\hat{\mathbf{l}}_z$ with eigenvalue m_μ, hence, the summation over m in Eq. (10) goes away. The only summation that we are left with is then over $n_\mu (\equiv 2n_{r\mu} + |m_\mu|$, where $n_{r\mu} = 0,1,2,\ldots,)$. Thus, we get

$$\chi_\mu(\mathbf{r}) = \sum_{n_\mu = |m_\mu|, |m_\mu|+2, \ldots} c^\mu_{n_\mu, m_\mu, 0} u_{n_\mu, m_\mu, 0}(\mathbf{r}). \tag{11}$$

Note that n_μ increases in steps of two, which comes from quantization. Tracing out the z coordinate, the density $\rho(r_\perp, \phi)$, the current $j_\phi(r_\perp, \phi)$, and the velocity $v_\phi(r_\perp, \phi)$ profiles in the x-y plane, for the quasi-2D system, turn out to be

$$\begin{aligned}\rho(r_\perp,\phi) &= \frac{\alpha_\perp^2}{\pi} e^{-\alpha_\perp^2 r_\perp^2} \sum_\mu \lambda_\mu \\ &\quad \times \left| \sum_{n_\mu = |m_\mu|, |m_\mu|+2, \ldots} c^\mu_{n_\mu, m_\mu, 0} \right. \\ &\quad \times \sqrt{\frac{(\frac{1}{2}[n_\mu - |m_\mu|])!}{(\frac{1}{2}[n_\mu + |m_\mu|])!}} \\ &\quad \left. \times (r_\perp \alpha_\perp)^{|m_\mu|} L^{|m_\mu|}_{(1/2)(n_\mu - |m_\mu|)}(r_\perp^2 \alpha_\perp^2) \right|^2 \\ &\equiv \rho(r_\perp),\end{aligned} \tag{12}$$

$$\begin{aligned}j_\phi(r_\perp,\phi) &= \sqrt{\frac{\hbar\omega_\perp}{m}} \left(\frac{1}{\alpha_\perp r_\perp} \right) \sum_\mu m_\mu \lambda_\mu |\chi_\mu(r_\perp,\phi)|^2 \\ &\equiv j_\phi(r_\perp),\end{aligned} \tag{13}$$

$$j_{r_\perp}(r_\perp,\phi) = j_z(r_\perp,\phi) = 0;$$

$$v_\phi(r_\perp,\phi)=\sqrt{\frac{\hbar\omega_\perp}{m}}\left(\frac{1}{\alpha_\perp r_\perp}\right)\sum_\mu m_\mu\lambda_\mu\frac{|\chi_\mu(r_\perp,\phi)|^2}{\rho(r_\perp,\phi)}$$
$$\equiv v_\phi(r_\perp), \tag{14}$$
$$v_{r_\perp}(r_\perp,\phi)=v_z(r_\perp,\phi)=0.$$

The density and the velocity profiles are presented in Figs. 2 and 3 for the single vortex state with $L_z=N$ for $N=15$. For completeness, we also give the circulation $\kappa(r_\perp)$ and the velocity curl profiles

$$\kappa(r_\perp)\equiv\oint_{r_\perp=\text{const}}\mathbf{v}\cdot d\mathbf{l}$$
$$=\int_0^{2\pi}v_\phi(r_\perp)r_\perp d\phi$$
$$=2\pi r_\perp v_\phi(r_\perp)=2\pi\frac{\hbar}{m}\sum_\mu m_\mu\lambda_\mu\frac{|\chi_\mu(r_\perp,\phi)|^2}{\rho(r_\perp,\phi)}, \tag{15}$$

$$\nabla\times\mathbf{v}=\frac{\hat{z}\omega_\perp}{\rho(r_\perp,\phi)}\sum_\mu\lambda_\mu\left(\frac{m_\mu}{r_\perp\alpha_\perp}-v_\phi\sqrt{\frac{m}{\hbar\omega_\perp}}\right)$$
$$\times\left[\chi_\mu^*\left(\sum_{n_\mu}c^\mu_{n_\mu,m_\mu,0}\{n_\mu\ u_{n_\mu,m_\mu,0}-\sqrt{(n_\mu-|m_\mu|)(n_\mu+|m_\mu|)}\ u_{n_\mu-2,m_\mu,0}\}\right)+\text{c.c.}\right]. \tag{16}$$

The expression for circulation as in Eq. (15) calls for some discussion. The circulation associated with each of the eigencomponents (χ_μ) of the one-particle density matrix is, of course, quantized as integral multiples of h/m for any closed path, and clearly can have no $r_\perp$ dependence for the circular paths chosen for our line integral. The expression, however, involves an average over different components χ_μ, and can, therefore, assume nonintegral values that vary with $r_\perp$ for the chosen circular path $r_\perp=$const. This reflects the radial variation of the relative fractional weights $m_\mu\lambda_\mu|\chi_\mu(r_\perp,\phi)|^2$ of the different fractions with $r_\perp$.

V. RESULTS AND DISCUSSION

The results and discussions given below refer to ^{87}Rb and the following choice of parameters [20]: $\lambda_z=\sqrt{8}$, $\omega_z/2\pi=220$ Hz, $a_\perp=1.222\mu m$, $a_{sc}=1000a_0$, where a_0 is the Bohr radius. Note that the scattering length a_{sc} chosen above is ten times that given in the above reference for ^{87}Rb. We have consciously chosen this to be so because it has been argued [6] that the relevant parameter in the problem under study here is (Na_{sc}/a_{ho}), and since in our calculation there is little room to further increase the value of N for reasons of computational resources required, we thought it appropriate to increase a_{sc} so as to get closer to the value of the parameter (Na_{sc}/a_{ho}) corresponding to the experimental situation. Here, we note in passing that many of the properties that we examined, like the condensate fraction and the critical angular velocities Ω_{ci}, were found to be varying smoothly as a_{sc} was varied between $1a_0$ and $1000a_0$(we will discuss some of these results in the text ahead). We present here the results for $N=15$ only in the angular momentum regime $0\leqslant L_z$

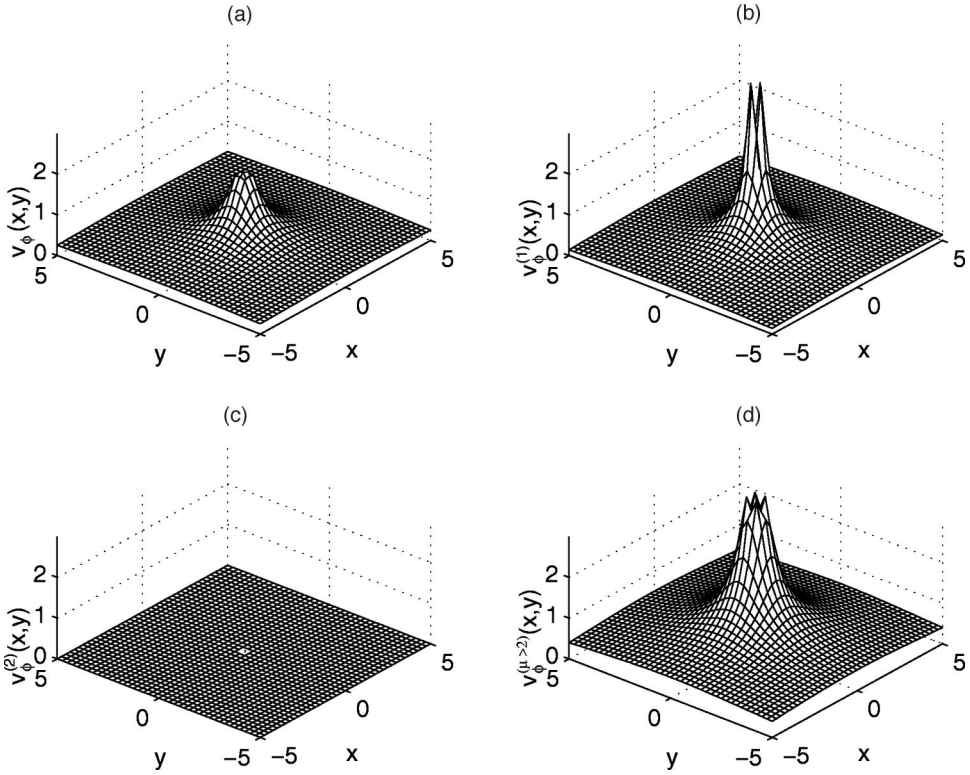

FIG. 3. Depicts the azimuthal velocity profile in units of $\sqrt{\hbar\omega_\perp/m}$ for (a) the total system $v_\phi(r_\perp)$, (b) the condensate fraction $v_\phi^{(1)}(r_\perp)$, (c) the nonrotating component $v_\phi^{(2)}(r_\perp)$, and (d) the remaining components $v_\phi^{(\mu>2)}(r_\perp)$ in the x-y plane. Distances are in units of $a_\perp$.

$\leqslant 3N$. We have, however, done the calculations for $N=6$, 8, 10, and $N=12$ also. First we note that we are always in the dilute gas limit here inasmuch as $N(a_{sc}/a_{ho})^3 \ll 1$, with $a_{ho} \equiv (a_\perp^2 a_z)^{1/3} = a_\perp \lambda_z^{-1/6}$. Further, we are also in the regime of moderate ($a_{sc}=1000a_0$) to very weak ($a_{sc}=1a_0$) interaction strength as the parameter Na_{sc}/a_{ho} is of order 1 or much less than 1 for the two regimes, respectively. Moreover, for $a_{sc}=1000a_0$, the healing length ξ [$\equiv(8\pi \bar{n} a_{sc})^{-1/2}$, with $\bar{n} \sim N/a_{ho}^3$, the mean particle density] $<$ the oscillator length a_{ho} $\sim$ the size of the system. Thus, our study for the above choice of parameters may be relevant to bulk systems.

The critical angular velocity Ω_{c1} for the single-vortex state ($L_z=N$) decreases for increasing value of N. Thus, for $a_{sc}=1000a_0$, it is $0.8849\omega_\perp$, $0.8679\omega_\perp$, and $0.8449\omega_\perp$ for $N=10$, 12, and 15, respectively. For a given N, the critical angular velocity Ω_{c1} is also found to decrease with increasing scattering length a_{sc}. Thus, for $N=15$, Ω_{c1} (in units of $\omega_\perp$) is found to be 0.9998, 0.9978, 0.9790, and 0.8449 for $a_{sc}=1a_0$, $10a_0$, $100a_0$, $1000a_0$, respectively. The condensate fraction (i.e., the largest eigenvalue λ_1 of the density matrix) for a given N and corresponding to the single vortex state ($L_z=N$), however, seems to be quite insensitive to a change in the scattering length in the weakly to the moderately interacting regime. Thus, for $L_z=N=15$ state and $a_{sc}=1a_0$, $10a_0$, $100a_0$, $1000a_0$, the condensate fractions (i.e., λ_1 values) are found to be 0.878 27, 0.878 26, 0.877 78, 0.870 69, respectively, i.e., the condensate fraction slowly decreases with increasing interaction. However, as we go over to the strongly interacting regime, the condensate begins getting strongly depleted. Thus, for $a_{sc}=10\,000a_0$, the condensate fraction for the single vortex state $L_z=N=15$ reduces to 0.7674. For higher vortex states like, say, $L_z=26$ and $L_z=2N=30$ for $N=15$, the condensate fractions are 0.5404, 0.5408, 0.5455, 0.5845 (slowly increasing) and 0.4187, 0.4182, 0.4167, 0.3996 (slowly decreasing), respectively, for $a_{sc}=1a_0$, $10a_0$, $100a_0$, $1000a_0$.

In Table I, we summarize our results for the ground state of the $N=15$ system in different subspaces of the total angular momentum L_z in the regime $0 \leqslant L_z \leqslant 3N$ for $a_{sc}=1000a_0$. As the system is rotated, a number of (total) angular momentum states are found to be stable at successively higher angular velocities Ω_{ci}, $i=1,2,\ldots$. We have also given the density-matrix eigenvalues $\{\lambda_\mu\}$ and the corresponding single-particle angular momentum quantum number $\{m_\mu\}$ for the largest three ($\lambda_1>\lambda_2>\lambda_3$) components. The single-particle angular momentum quantum number m_1, corresponding to the largest eigenvalue λ_1, is taken to be the vorticity of the condensate. We note that, corresponding to each of the stable ground states of the rotating system, namely, $L_z=15$, 26, 30, 33, 35, 36, 45, . . . for $N=15$, the second largest fraction is found to be nonrotating, i.e., $m_2=0$. Hence, particles driven out of the condensate by the centrifugal force prefer to go to the zero angular momentum ($m=0$) state.

Figure 1 gives the L_z-Ω phase diagram, or the stability line. One can readily identify the successive critical angular velocities $\{\Omega_{ci},\ i=0,1,2,\ldots\}$ for the transition from one stable state to another stable state. Several points are to be noted here. The nonintegral values for the angular momentum per particle clearly indicates the incomplete condensation, i.e., the fact that more than one eigenvalues $\{\lambda_\mu\}$ of the reduced density matrix are nonzero. This is, however, not to be taken as the fragmented condensate [21] as in the context of a spatially homogeneous bosonic system with attractive interaction, but merely as depletion of the condensate fraction due to the interaction and the rotation. Also, we have observed that the critical angular velocity Ω_{ci} decreases monotonically with increasing repulsive interaction and the particle number. This can be readily understood physically from the expression in Eq. (9) for the critical angular velocity $\Omega_{ci} \equiv \Omega_{ci}(L_z, \Lambda_2)$ if one remembers that the nonrotating ($L_z=0$ angular momentum) state is more compact and, therefore, has its energy raised (because of the repulsive interaction) relative to the expanded higher angular momentum states. More importantly, however, our critical angular velocity Ω_{c1} for a given N, is systematically greater than the nonvariational value based on the yrast-like state [14,15,12,13]. We expect this to be due to our more accurate and, therefore, lower variational ground-state energies.

In Fig. 2(a) we have plotted the total density profile $\rho(r_\perp)$ for the $L_z=N$ single-vortex state of the system. We have also plotted separately the density profiles for the different components of the density: $\lambda_1|\chi_1(\mathbf{r})|^2 \equiv \rho^{(1)}(r_\perp,\phi)$ corresponding to the largest eigenvalue $\lambda_1(=0.870\,69)$ in Fig. 2(b), $\lambda_2|\chi_2(\mathbf{r})|^2 \equiv \rho^{(2)}(r_\perp,\phi)$ corresponding to the second largest eigenvalue $\lambda_2(=0.065\,76)$ in Fig. 2(c), and $\rho^{(\mu>2)}(r_\perp,\phi)$ corresponding to the remaining components in Fig. 2(d) obtained from the one-particle reduced density matrix

$$\rho_1(\mathbf{r},\mathbf{r}') = \underbrace{\lambda_1 \chi_1^*(\mathbf{r})\ \chi_1(\mathbf{r}')}_{\substack{\text{the condensate}\\ \text{with } m_1=1}} + \underbrace{\lambda_2 \chi_2^*(\mathbf{r}) \chi_2(\mathbf{r}')}_{\substack{\text{the nonrotating component with } m_2=0}} + \underbrace{\sum_{\mu=3} \lambda_\mu \chi_\mu^*(\mathbf{r})\ \chi_\mu(\mathbf{r}')}_{\substack{\text{the remaining components}\\ \text{comprising of } m_\mu,\ \mu>2}}$$

where, as earlier, m_μ is the single-particle angular momentum quantum number associated with the μth component of the density matrix. As we go to higher Ω, the condensate depletes-with the nonrotating component $\rho^{(2)}(r_\perp,\phi)$ and the remaining components $\rho^{(\mu>2)}(r_\perp,\phi)$ become more pronounced (as can also be seen from Table I). We would like to

TABLE I. Gives the largest three eigenvalues $\lambda_1 > \lambda_2 > \lambda_3$ and the corresponding single-particle angular momentum eigenvalues m_1, m_2, and m_3 in the one-particle reduced density-matrix $\rho(\mathbf{r},\mathbf{r}') = \Sigma_\mu \lambda_\mu \chi_\mu^*(\mathbf{r})\chi_\mu(\mathbf{r}')$ for the ground state of the rotating BEC, in given subspaces of the total angular momentum L_z. Also given are the ground-state energies $E_0^{lab}(L_z)$ in the laboratory frame and the critical angular velocities Ω_{ci} corresponding to the stable ground states of the rotating system in the angular momentum regime $0 \leqslant L_z \leqslant 3N$.

			Largest three condensate fractions ($\lambda_1 > \lambda_2 > \lambda_3$)					
			Largest		2nd largest		3rd largest	
L_z	$E_0^{lab}(L_z)$	$\Omega_{ci}, i=0,1,\ldots,$	m_1	λ_1	m_2	λ_2	m_3	λ_3
0	41.18837	0	0	0.9943	1	0.0021	−1	0.0021
1	42.19021		0	0.9251	1	0.0693	−1	0.0036
2	42.99052		0	0.9198	2	0.0586	1	0.0181
3	43.79210		0	0.9133	3	0.0531	1	0.0181
4	44.73324		0	0.8268	1	0.0925	2	0.0543
5	45.55314		0	0.8128	2	0.0741	1	0.0717
6	46.38548		0	0.7976	3	0.0792	1	0.0765
7	47.25794		0	0.6948	1	0.1737	2	0.0914
8	48.08941		0	0.6520	1	0.2007	2	0.1002
9	48.92517		0	0.5878	1	0.2618	2	0.1046
10	49.75782		0	0.5114	1	0.3377	2	0.1164
11	50.58520		0	0.4391	1	0.4119	2	0.1189
12	51.41082		1	0.5015	0	0.3583	2	0.1166
13	52.23442		1	0.6055	0	0.2701	2	0.1072
14	53.05612		1	0.7299	0	0.1717	2	0.0875
15	53.86234	0.8449	1	0.8707	0	0.0658	2	0.0574
16	54.86287		1	0.7072	2	0.1567	0	0.1197
17	55.84557		1	0.6143	2	0.1837	0	0.1543
18	56.72501		1	0.7204	2	0.1086	0	0.0985
19	57.69445		1	0.5298	2	0.2348	0	0.1593
20	58.64083		2	0.3683	1	0.2937	0	0.2541
21	59.56022		1	0.4084	2	0.2839	0	0.1880
22	60.48086		2	0.4876	0	0.2846	1	0.1303
23	61.43733		2	0.4410	0	0.2272	1	0.2002
24	62.33085		2	0.5453	0	0.2567	1	0.0805
25	63.31524		2	0.4498	0	0.2042	1	0.1677
26	64.20739	0.9405	2	0.5845	0	0.2138	4	0.0879
27	65.22391		2	0.4518	0	0.2065	3	0.1797
28	66.11546		2	0.5858	0	0.1773	4	0.1088
29	67.13036		2	0.3556	3	0.2596	0	0.2168
30	68.00749	0.9500	2	0.3996	0	0.2001	4	0.1463
31	68.96896		2	0.2725	0	0.2255	3	0.1883
32	69.93098		3	0.3235	0	0.2506	2	0.1905
33	70.88661	0.9597	3	0.4393	0	0.2553	2	0.1168
34	71.86427		3	0.2384	0	0.2210	2	0.2106
35	72.81314	0.9633	3	0.2733	0	0.2304	2	0.1701
36	73.78031	0.9672	3	0.4723	0	0.2086	4	0.1160
37	74.77086		3	0.2920	0	0.2178	2	0.1608
38	75.74022		3	0.3326	0	0.2193	4	0.1648
39	76.69427		4	0.2501	3	0.2272	0	0.2252
40	77.66436		4	0.4148	0	0.2758	5	0.1081
41	78.68052		4	0.2941	0	0.2579	5	0.1916
42	79.64666		4	0.2256	0	0.2150	3	0.2113
43	80.60356		4	0.3664	0	0.2159	5	0.1554
44	81.56135		4	0.5041	0	0.2341	5	0.1101
45	82.49866	0.9687	3	0.2538	0	0.2093	4	0.1980

emphasize here that for a confined, finite, rotating system of interacting bosons, the one-particle reduced density matrix as decomposed above according to the singe-particle angular momentum value is an unambiguous description of the system.

Figure 3 depicts the velocity profiles $v_\phi(r_\perp,\phi)$ for the total system in (a), $v_\phi^{(1)}(r_\perp,\phi)\equiv[(m_1/\alpha_\perp r_\perp)\sqrt{\hbar\omega_\perp/m}]$ for the condensate in (b), $v_\phi^{(2)}(r_\perp,\phi)\equiv[(m_2/\alpha_\perp r_\perp)\sqrt{\hbar\omega_\perp/m}]$ for the non-rotating component in (c), and $v_\phi^{(\mu>2)}(r_\perp,\phi)$ for the remaining components in (d).

As can readily be seen, for circular paths of radii $r_\perp$ in the x-y plane, the condensate fraction has an integral circulation $\kappa^{(1)}(r_\perp)\equiv m_1 h/m$ and is constant over space.

In conclusion, our many-body variational calculation for an admittedly finite number ($N\leqslant 15$) of particles explicitly resolves the structure of the rotating BEC at $T=0$ in terms of the various components of the reduced one-particle density matrix. Further work is in progress to consider spin-1 Bose particles, where we expect qualitative changes in the structure of the rotating BEC. In particular, we expect a dramatic increase in the critical angular velocities because of the spin-polarization drag effect inasmuch as the angular momentum may be absorbed preferentially in the spin rather than the orbital degrees of freedom without costing kinetic energy. This could lead to spin polarization due to the rotation of the trap [22,23]. We expect this effect to be more pronounced here than in a classical rotating system.

ACKNOWLEDGMENT

One of us (M.A.H.A.) would like to thank Professor R. Nityananda and Professor R. Srinivasan for useful discussions.

[1] M. H. Anderson, J. R. Ensher, M. R. Matthews, C. E. Wieman, and E. A. Cornell, Science **269**, 198 (1995).
[2] K. B. Davis, M. O. Mewes, M. R. Andrews, N. J. van Druten, D. S. Durfee, D. M. Kurn, and W. Ketterle, Phys. Rev. Lett. **75**, 3969 (1995).
[3] C. C. Bradley, C. A. Sackett, J. J. Tollett, and R. G. Hulet, Phys. Rev. Lett. **75**, 1687 (1995).
[4] D. G. Fried, T. C. Killian, L. Willmann, D. Landhuis, S. C. Moss, D. Kleppner, and T. J. Greytak, Phys. Rev. Lett. **81**, 3811 (1998).
[5] G. Baym and C. J. Pethick, Phys. Rev. Lett. **76**, 6 (1996).
[6] F. Dalfovo, S. Giorgini, L. P. Pitaevskii, and S. Stringari, Rev. Mod. Phys. **71**, 463 (1999).
[7] See, Proceedings of the International School of Physics ''Enrico Fermi,'' Course CXL, 1999, edited by M. Inguscio, S. Stringari, and C. E. Wieman (IOS Press, Netherlands, 1999).
[8] S. Inouye, M. R. Andrews, J. Stenger, H.-J. Miesner, D. M. Stamper-Kurn, and W. Ketterle, Nature (London) **392**, 351 (1998).
[9] M. R. Matthews, B. P. Anderson, P. C. Haljan, D. S. Hall, C. E. Wieman, and E. A. Cornell, Phys. Rev. Lett. **83**, 2498 (1999).
[10] K. W. Madison, F. Chevy, W. Wohlleben, and J. Dalibard, Phys. Rev. Lett. **84**, 806 (2000).
[11] M. R. Andrews, C. G. Townsend, H.-J. Miesner, D. S. Durfee, D. M. Kurn, and W. Ketterle, Science **275**, 637 (1997).
[12] G. F. Bertsch and T. Papenbrock, Phys. Rev. Lett. **83**, 5412 (1999).
[13] N. K. Wilkin and J. M. F. Gunn, Phys. Rev. Lett. **84**, 6 (2000).
[14] D. A. Butts and D. S. Rokhsar, Nature (London) **397**, 327 (1999).
[15] B. Mottelson, Phys. Rev. Lett. **83**, 2695 (1999).
[16] V. Fock, Z. Phys. **47**, 446 (1928).
[17] C. G. Darwin, Proc. Cambridge Philos. Soc. **27**, 86 (1930).
[18] See cond-mat/0011212, section II, which is an expanded version of our current work where we have examined the mechanical stability of a harmonically confined particle of charge q in an external uniform magnetic field **B** and an externally impressed rotation $\mathbf{\Omega}$ along the z axis, according as $(\zeta_\perp+\varsigma)\times(\zeta_\perp-\varsigma)$ is negative, zero or positive, where $\zeta_\perp$ and ς are as defined in the text. For the special case of $\zeta_\perp=\varsigma$, we obtain a staircase of degenerate levels similar to Landau ones.
[19] E. R. Davidson, J. Comput. Phys. **17**, 87 (1975).
[20] F. Dalfovo and S. Stringari, Phys. Rev. A **53**, 2477 (1996).
[21] P. Nozieres and D. Saint James, J. Phys. (Paris) **43**, 1133 (1982).
[22] E. T. Jaynes, Phys. Rev. **106**, 620 (1957).
[23] N. Agarwal and N. Kumar (unpublished).